Supplementary Information

Gram-scale synthesis of aggregation-caused quenching-resistant red-emissive carbon dots for potential applications

Ashok Kumar[a] Kanchan Negi[a] and Sumanta Kumar Sahu[a*]

[a]Department of Chemistry and Chemical Biology, Indian Institute of Technology (ISM), Dhanbad 826004, Jharkhand, India.

*Corresponding author. E-mail: sumantchem@gmail.com, sksahu@iitism.ac.in;

Fax: +91 326-2307772; Tel: +91 3262235936, +91 7631042241

CONTENTS:

1. XRD pattern of R-CDs.

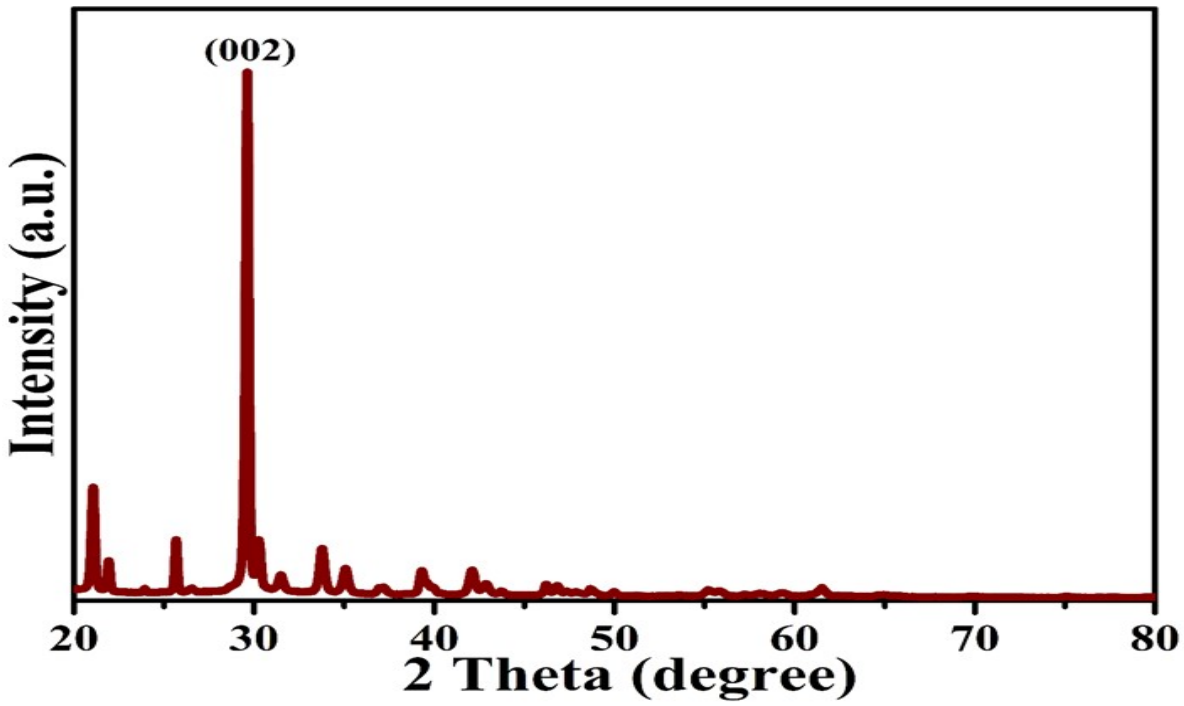

Figure S1. XRD pattern of R-CDs.

2. TGA curve of the R-CDs.

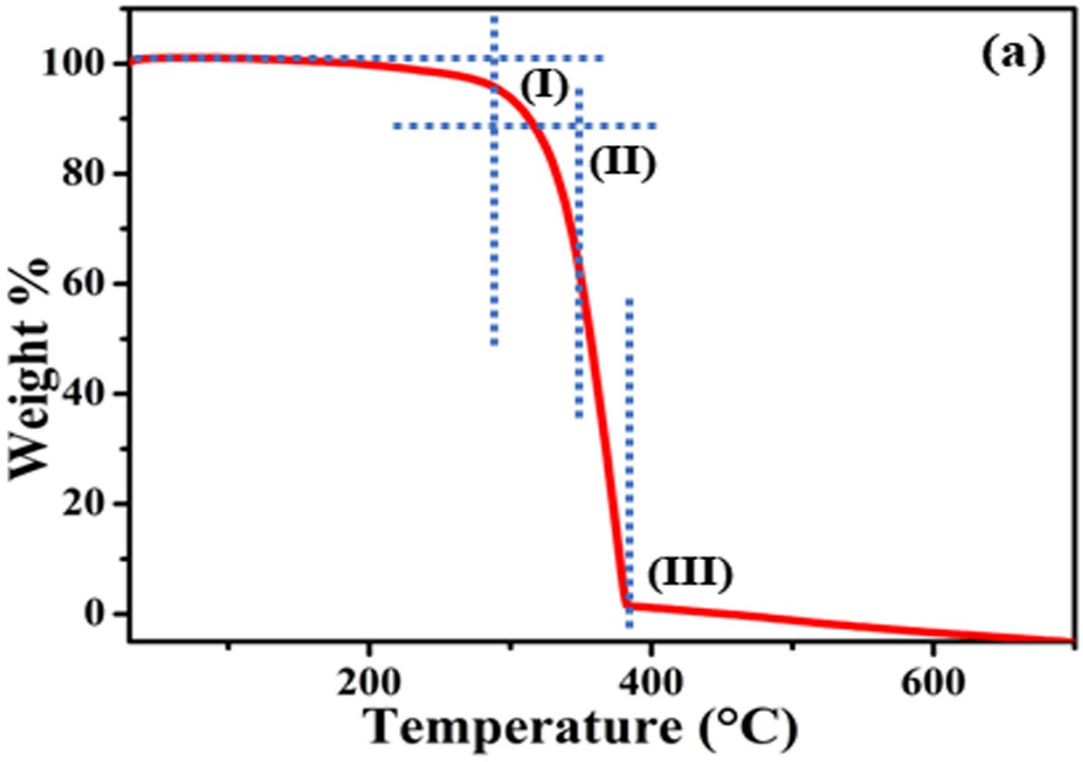

Figure S2. TGA curve of R-CDs.

3. The luminous activity of composite films.

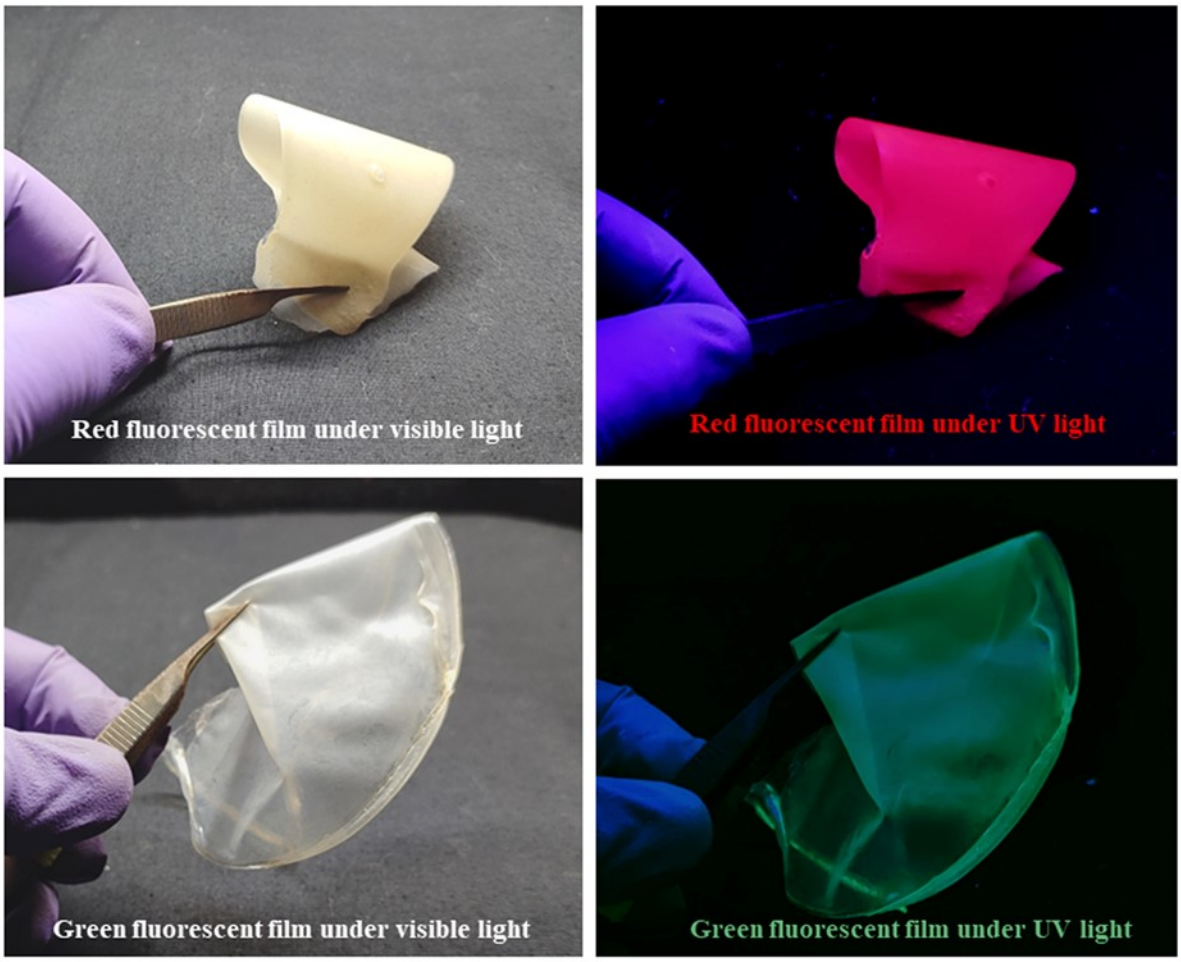

Figure S3. The luminous activity of R-CDs and G-CDs composite films by using visible and UV light.

4. The optical characteristics of polymer composite films.

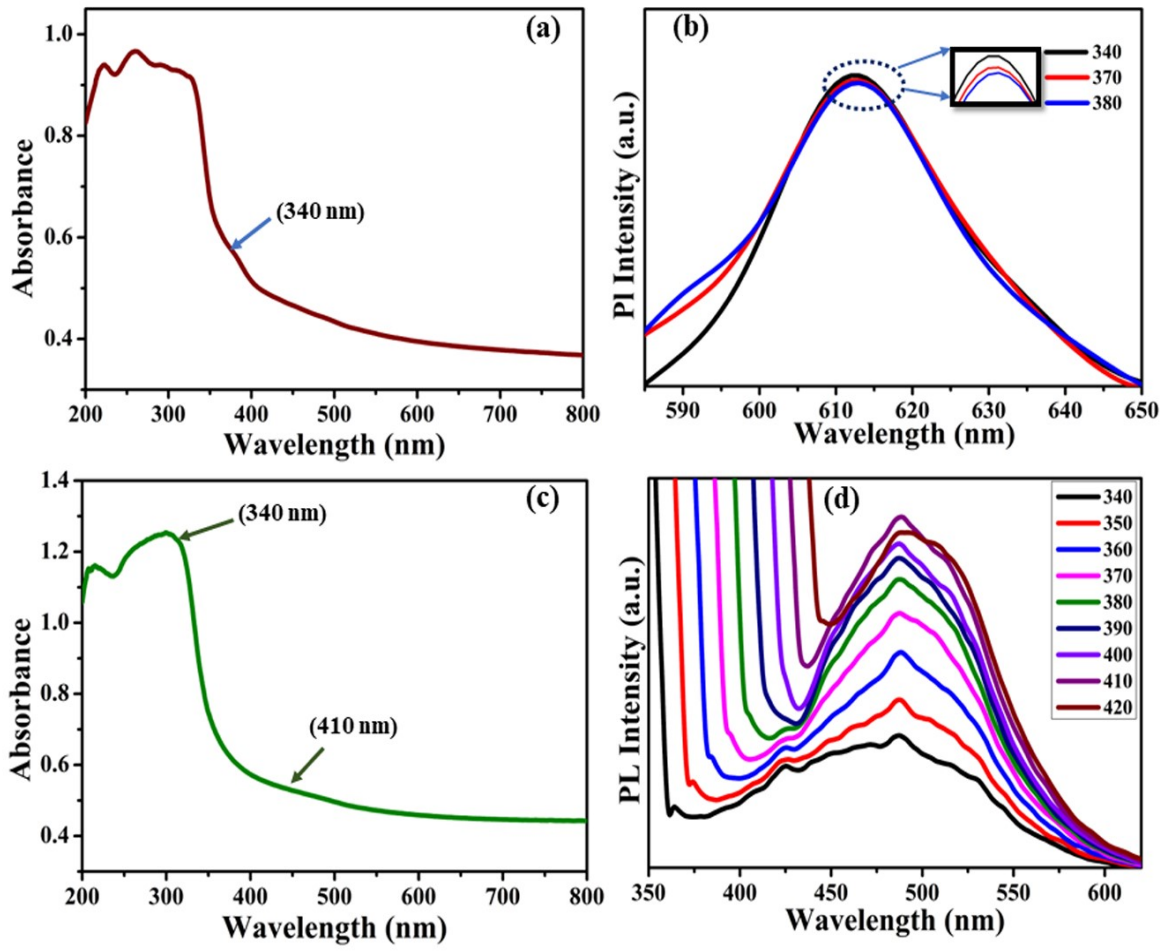

Figure S4. The optical behavior of the polymeric composite film: (a) the UV visible absorbance spectrum of R-CDs/PVA composite film (b) PL spectra of R-CDs/PVA (c) the UV visible absorbance spectrum of G-CDs/PVA composite film (b) PL spectra of G-CDs/PVA

5. Latent fingerprints developed on different surfaces and their luminous activity in UV and visible light.

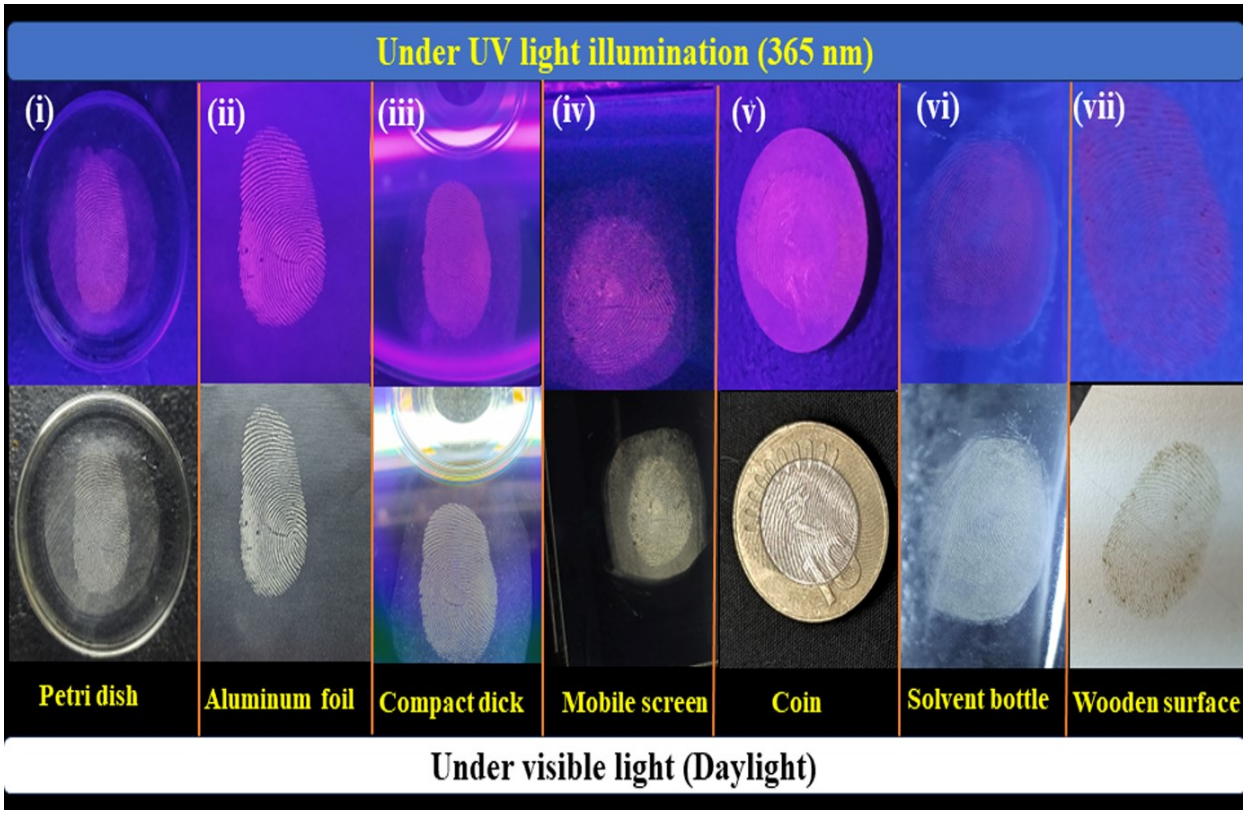

Figure S5. Latent fingerprint images developed with R-CDs and irradiated with 365 nm UV and visible light, the developed fingerprints on (i) a glass petri dish, (ii) aluminum foil, (iii) a compact disc glossy face (iv) mobile phone screen (v) coin (vi) plastic solvent bottle, and (vii) wooden surface.

6. Photobleaching and photostability studies of R-CDs.

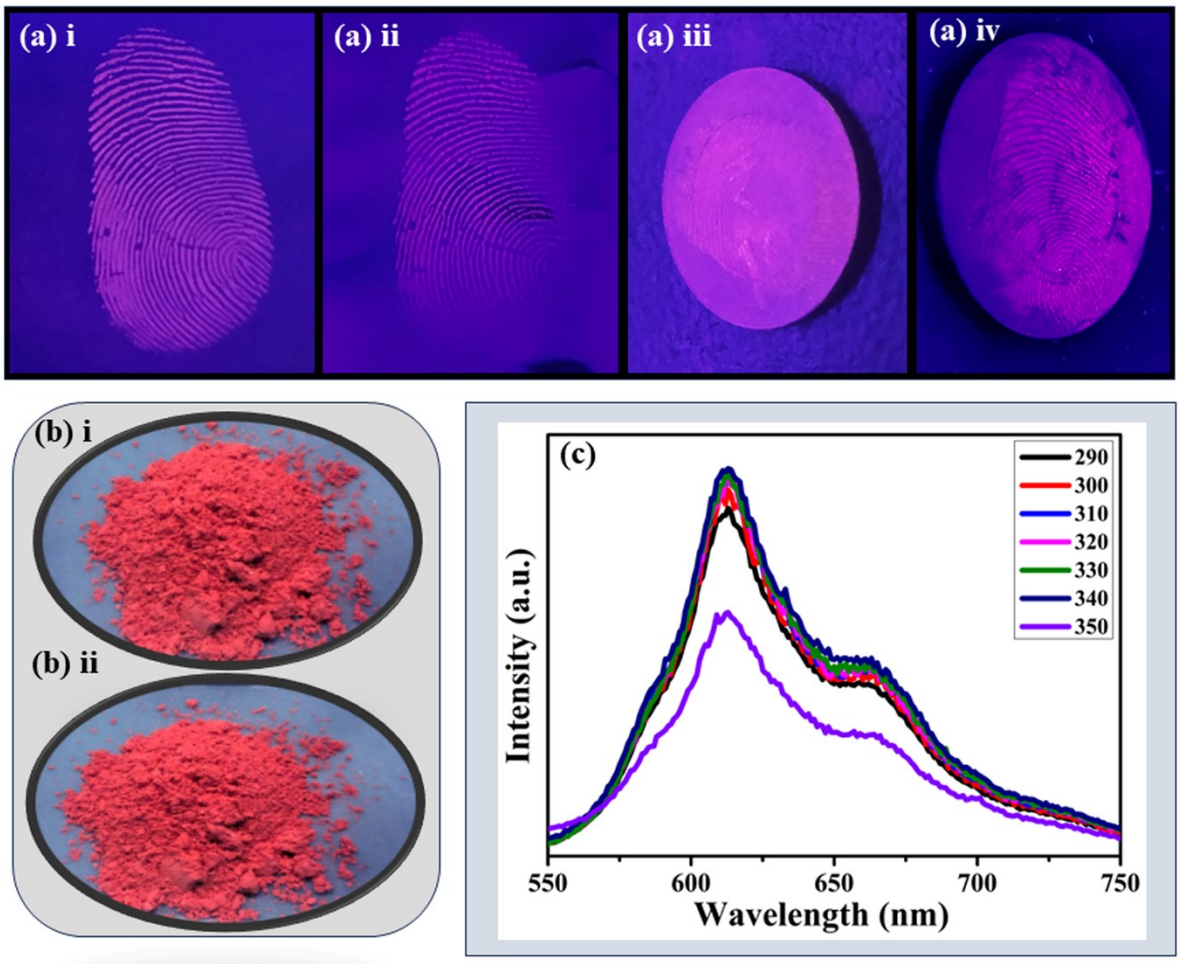

Figure S6. (a-i and a-iii) freshly developed fingerprints, and (a-ii and a-iv) after 12 weeks of storage (b-i) before irradiation under UV light, and (b-ii) after 1 hour of UV irradiation (c) the fluorescence emission spectra after three months of storage.

7. Development of fluorescent ink images and characters.

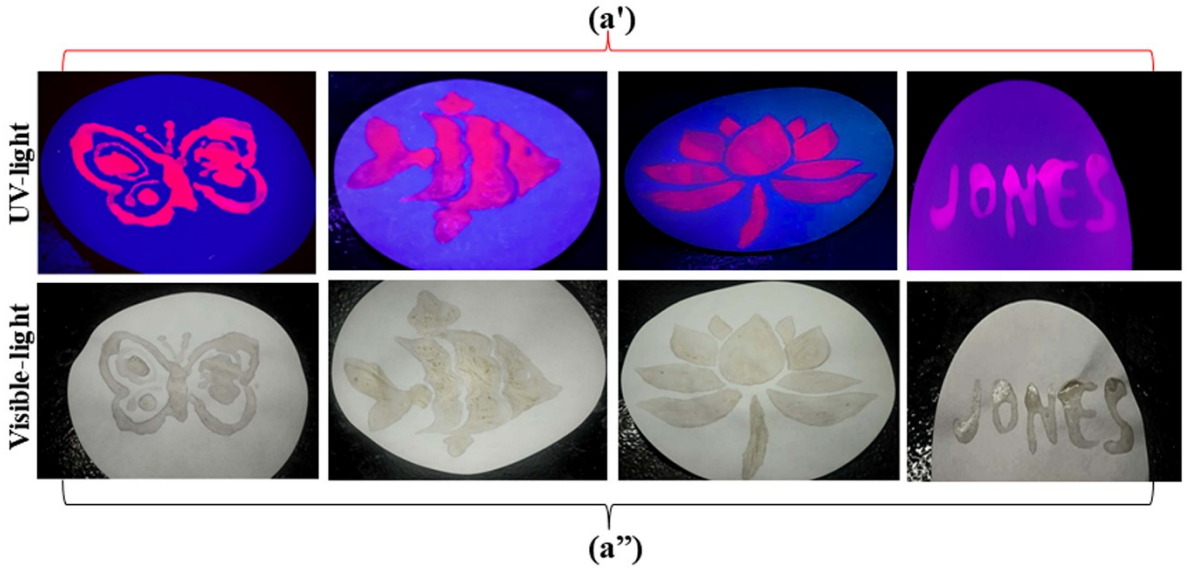

Figure S7. (a') fluorescent ink images and characters on commercial filter paper after 365 UV-light illumination, and (a") visible light.

8. Confocal fluorescence images of HEK293T cell lines.

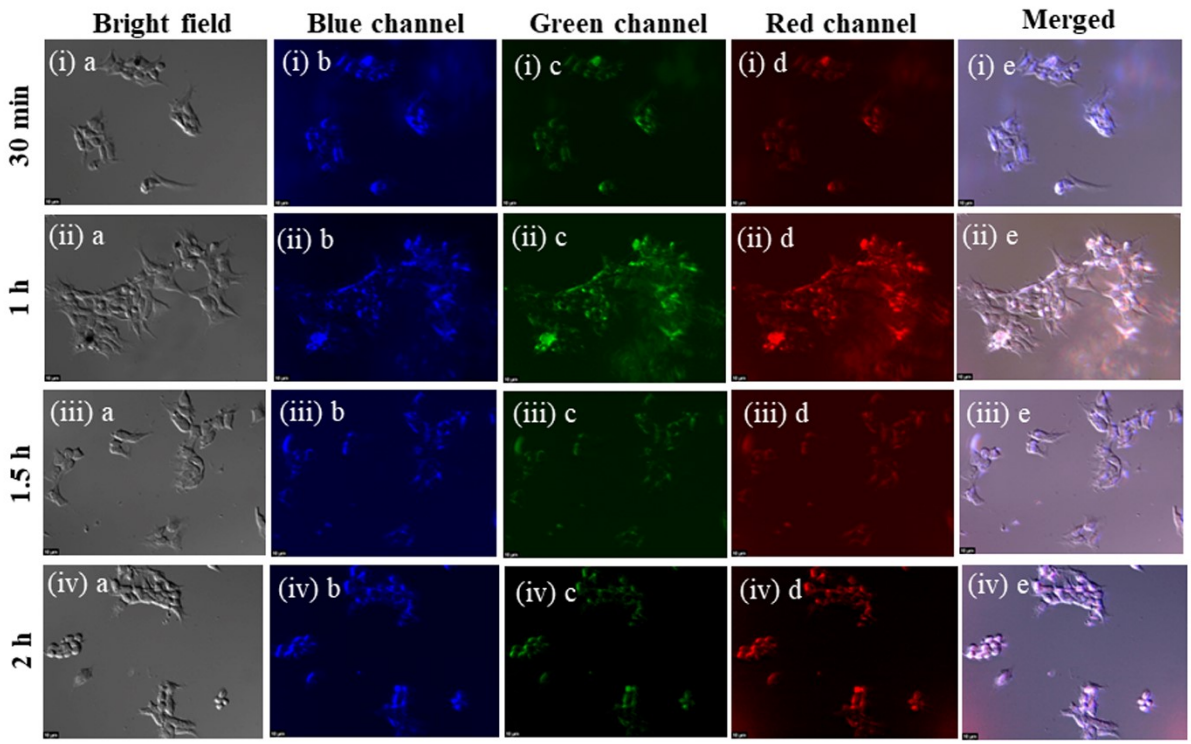

Figure S8. Confocal fluorescence images of HEK293T cell lines, cells treated with R-CDs (25 μg mL^{-1}) for changed time intervals (i) 30 min, (ii) 1 h, (iii) 1.5 h, (iv) 2 h, and different channels (a) bright field (b) blue channel (c) green channel (d) red channel (e) merged (the scale bar is 10 μm).

9. XPS survey of RTP-CDs.

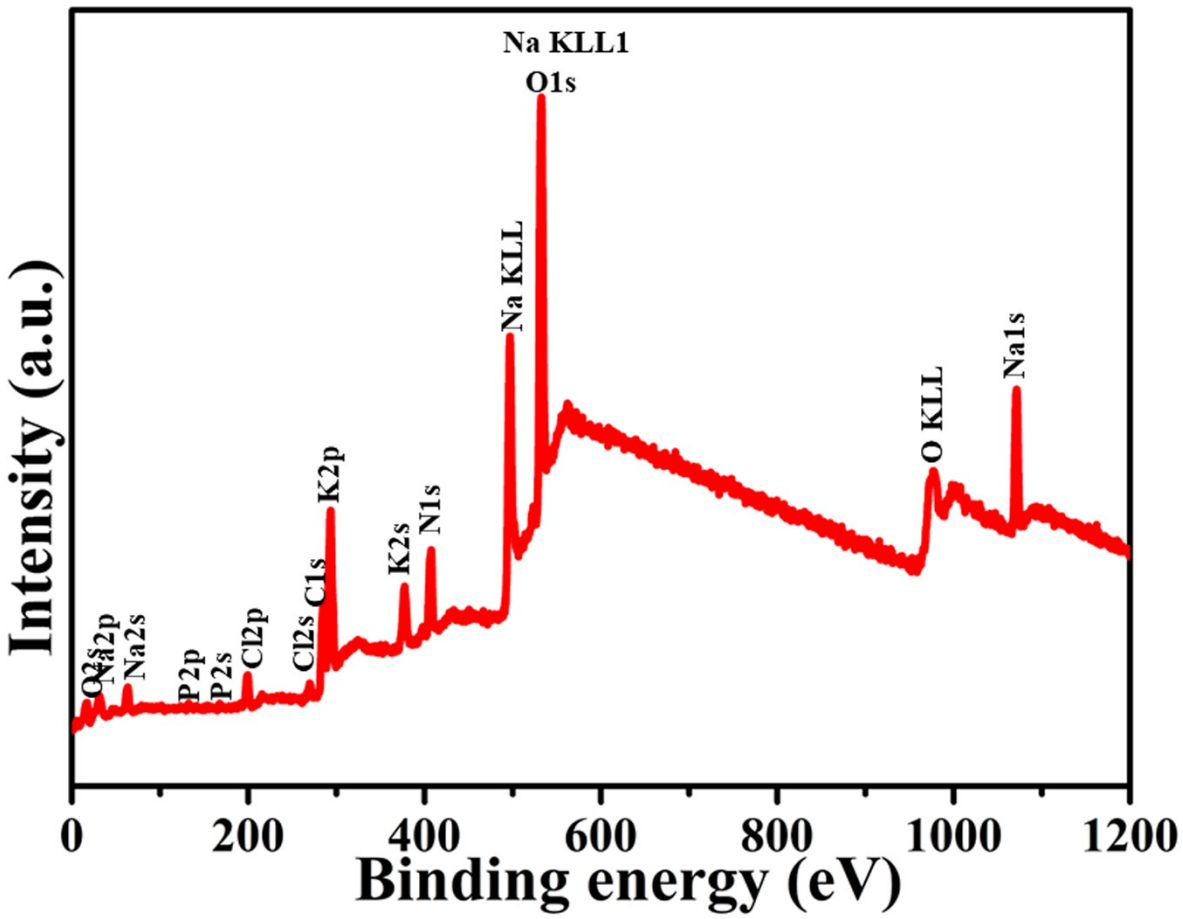

Figure S9. XPS survey of the synthesized RTP-CDs.

Table 1. Summary of some reported carbon dot-based WLEDs with CCT, CIE, and CRI.

CCT	CIE	CRI	References
5610 K	(0.33, 0.33)	92	[1]
5643 K	(0.31, 0.29)	87	[2]
6987 K	(0.30, 0.35)	83	[3]
3723 K	(0.39, 0.37)	91	[4]
5612 K	(0.33, 0.33)	89	[5]
7694 K	(0.29, 0.33)	83	[6]
4033 K	(0.38, 0.38)	**96**	**[This work]**

Table S1. Summary of some reported carbon dot-based WLEDs with CCT, CIE, and CRI.

Table 2. Elemental compositions table for RTP-CDs and R-CDs.

Elemental compositions of RTP-CDs.

Elements	O	C	N	Na	K	Cl	P	N/C	O/C
%	49.1	18.6	11.5	10.1	7.9	2.2	0.6	0.61	2.63

Elemental compositions of R-CDs.

Elements	O	C	N	S	N/C	O/C
%	22.56	66.70	10.55	0.19	0.15	0.33

Table S2. Elemental compositions of RTP-CDs and R-CDs.

10. High-resolution deconvolution spectra of C1s and O1s in RTP-CDs.

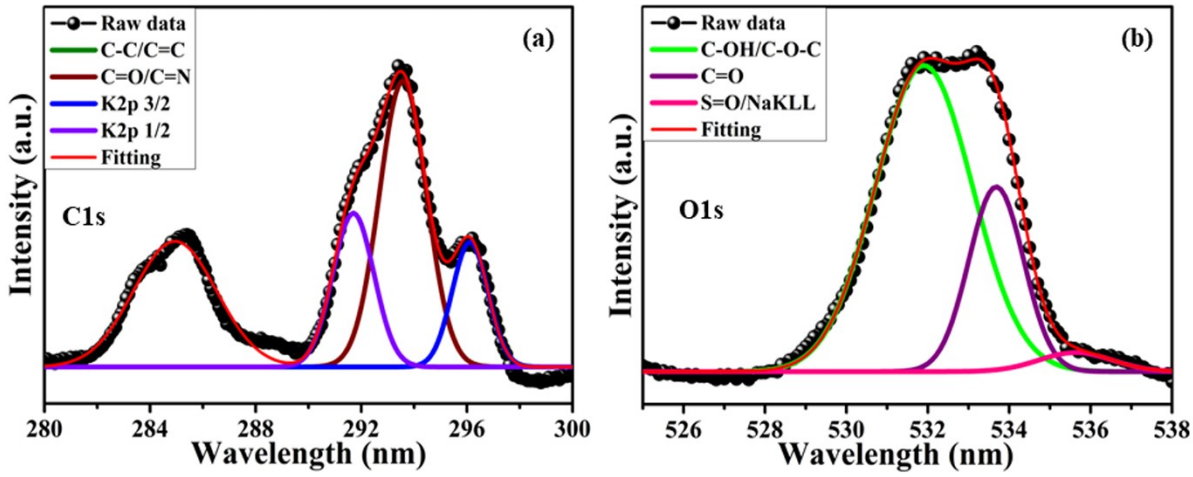

C1s	RTP-CDs
C-C/C=C	6238
C=O/C=N	8084

O1s	RTP-CDs
C-OH/C-O-C	20710
C=O	7034

Figure S10. XPS high-resolution deconvolution spectra of C1s and O1s and corresponding area values in the table.

11. The digital photograph of phosphorescent materials at different time intervals.

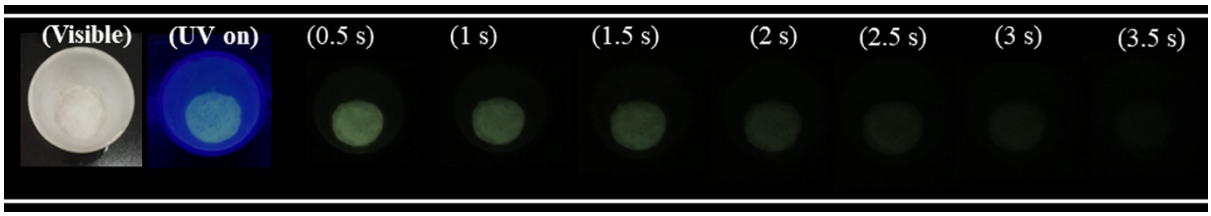

Figure S11. The digital photograph of RTP-CDs at diverse time intermissions with visible light on, UV source on and off.

12. The captured PL spectra at different currents and constant voltage.

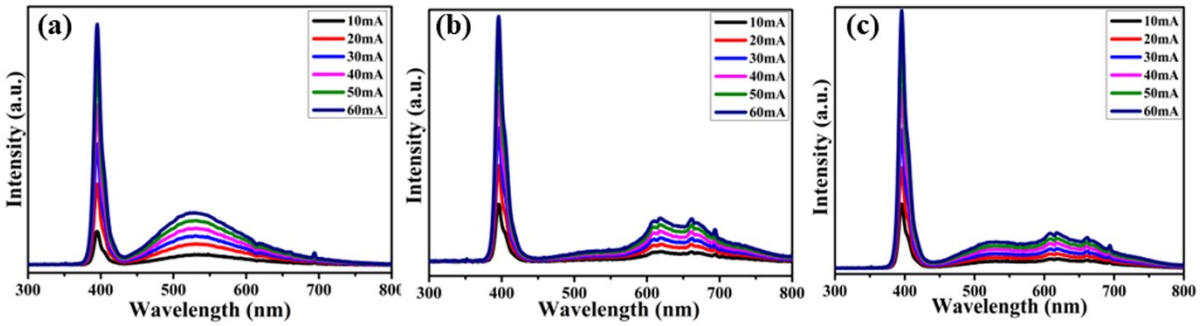

Figure S12. The PL emission spectra of the (a) G-CDs/PVA (b) R-CDs/PVA, and (c) WLEDs at different currents and a constant voltage of 4.5 V.

The preparation and characterizations of G-CDs.

A specific amount of R-CDs was dissolved in 20 ml ultrapure water and sonicated with a sonicator bath for 30 minutes. After the sonication time, the pH was adjusted from 7.4 (ultrapure water) to 12 using 0.1 M NaOH solution, we got G-CDs. We checked the optical characteristics of G-CDs via UV-vis absorbance and fluorescence spectroscopy. **Figure S13(a)** exhibits the UV-vis absorption spectrum. The UV-visible absorbance shows two peaks at 300 and one small peak at 340 nm, corresponding to the π-π* transitions of the C=C bonds and n-π* transitions of C=O/C=N/C=S bonds. Again, to know the emission of G-CDs we checked the fluorescence spectra of the G-CDs upon various excitation wavelengths. **Figure S13(b)** depicts the fluorescence spectra of G-CDs. The PL spectra show that the highest emission occurs at 455 nm under the 340 nm optimum excitation. The PL emission peak was shifted to a higher wavelength with the increase of excitation wavelength, this phenomenon is plausible due to the presence of diverse particle sizes present in the G-CDs solution. Furthermore, FTIR spectroscopy and XPS measurements were performed to analyze the surface structure and functional groups of the CDs. **Figure S13(c)** represents the FTIR

spectrum of the G-CDs. A broad, prominent peak appears in this spectrum between 3000 and 3500 cm^{-1}, showing the existence of a large number of O-H/N-H groups on the surface of CDs. [3]

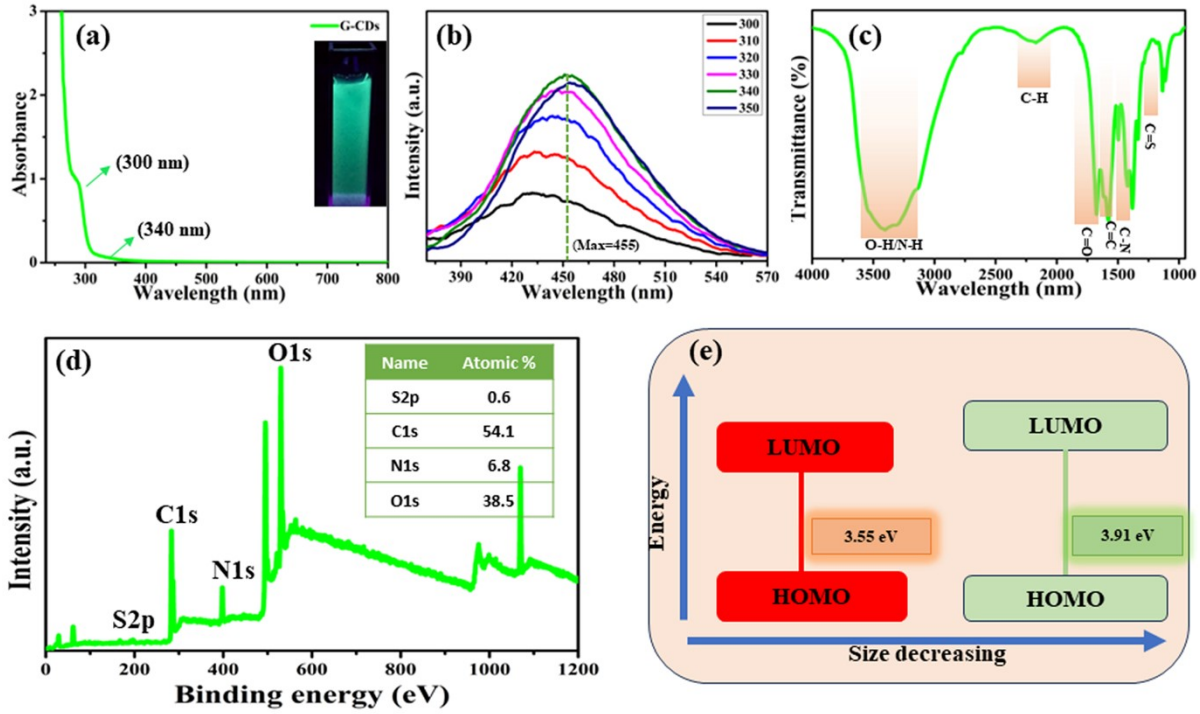

Figure S13. (a) UV-visible absorbance spectrum of G-CDs (b) PL spectra of G-CDs (c) FTIR spectrum of G-CDs (d) XPS survey of the G-CDs [Inset: Atomic % of the elements] (e) HOMO-LUMO diagram of the R-CDs and G-CDs.

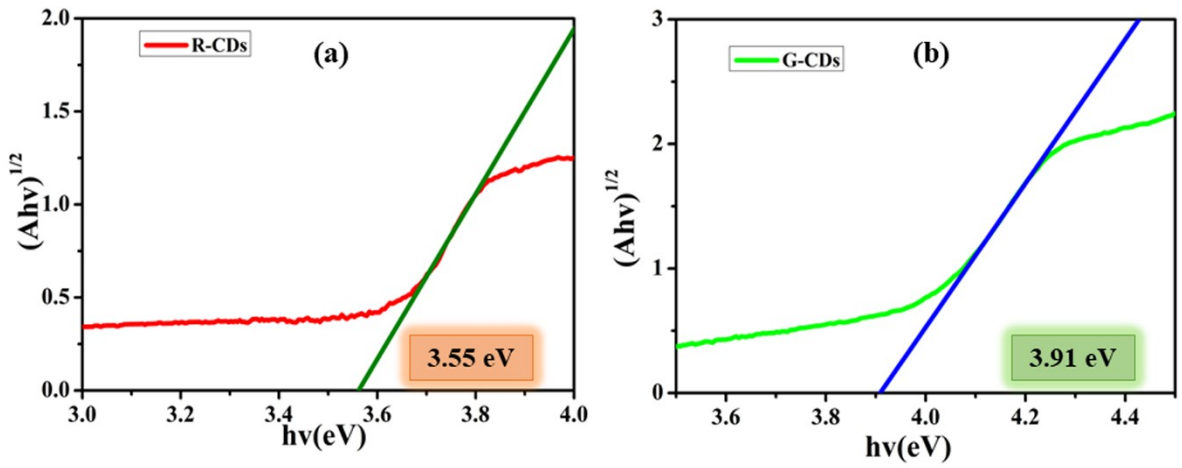

Figure S14. (a) Band gap of the R-CDs, and (b) G-CDs.

The absorption peaks at 2184, 1680, 1577, 1379, and 1272 cm^{-1} were attributed to the stretching vibrations of C-H, C=O, C=C, C–N, and C=S groups, respectively. [3-6] These functional groups show that the various functional groups were present on the surface of G-CDs which govern their hydrophilicity and good stability in aqueous solutions. Additionally, X-ray photoelectron spectroscopy (XPS) was utilized to confirm these chemical compositions of G-CDs. The atomic proportions of C, N, O, and S elements were revealed to be 54.1%, 6.8%, 38.5%, and 0.6%, respectively, in a full survey scan spectra of the XPS (**Figure S13(d)**). Now, we compare R-CDs with G-CDs using FTIR and XPS measurements. **Table S2** shows the atomic percentage of both CDs. Here, we see that the percentage of oxygen is increased in the G-CDs and the nitrogen percentage is decreased. This phenomenon proves that some of the bonds containing nitrogen functional groups are converted into oxygen-containing groups. Further, we see that the FTIR spectrum of R-CDs gives a small intensity peak whereas the FTIR spectrum of G-CDs shows a broad, prominent peak which confirms the high number of hydroxyl groups present on the surface of G-CDs. The possible explanation behind this formation of G-CDs is the disruption of the highly conjugated anhydride system of R-CDs in the presence of excess hydroxyl ions at pH 12. This disruption caused to change in the surface state and widened the HOMO-LUMO gap, which resulted in the green color emission. The HOMO-LUMO gap is calculated based on UV-visible spectrum which is shown in **Figure S14(a-b)**, and the detailed diagram is shown in **Figure S13(e)**.

References: -

1. Y. Zhai, Y. Wang, D. Li, D. Zhou, P. Jing, D. Shen and S. Qu, *J. Colloid Interface Sci.*, 2018, **528**, 281-288.

2. Z. Sun, F. Yan, J. Xu, H. Zhang and L. Chen, *Nano Res.*, 2022, **15**, 414-422.

3. X. Feng, K. Jiang, H. Zeng and H. Lin, *Nanomaterials (Basel)*, 2019, **9**, 725.

4. Q. Han, W. Xu, C. Ji, G. Xiong, C. Shi, D. Zhang, W. Shi, Y. Jiang and Z. Peng, *ACS Appl. Nano Mater.*, 2022, **5**, 15914-15924.

5. W. Cai, T. Zhang, M. Xu, M. Zhang, Y. Guo, L. Zhang, J. Street, W.-J. Ong and Q. Xu, *J. Mater. Chem. C Mater. Opt. Electron. Devices*, 2019, **7**, 2212-2218.

6. J. Xu, Y. Miao, J. Zheng, H. Wang, Y. Yang and X. Liu, *Nanoscale*, 2018, **10**, 11211-11221.

15. Temperature and ratio optimization studies of R-CDs.

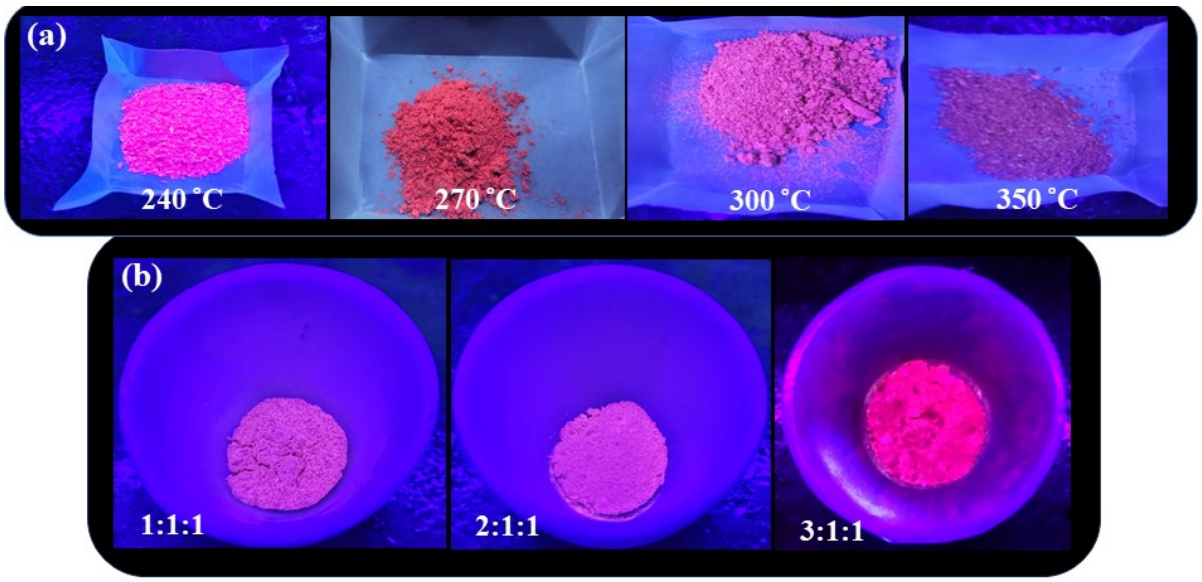

Figure S15. Temperature and ratio optimization studies of R-CDs (a) R-CDs were synthesized at different temperatures such as 240 C, 270 ℃, 300 ℃, and 350 ℃, here, we see

that at lower temperatures (240 C) the precursors are not properly calcined whereas at higher temperatures 300 and 350 C carbon depositions increase. (b) different ratio optimizations of precursors.